DESIGN AND EXPERIMENTAL ANALYSIS OF HIGH-SPEED FEED PUMP FOR SMALL-SCALE ORC

Petri Sallinen[1]*, Antti Uusitalo[1], Juha Honkatukia[1], Jonna Tiainen[1], Teemu Turunen-Saaresti[1]

[1]LUT University, Lappeenranta, Finland
*Corresponding Author: petri.sallinen@lut.fi

ABSTRACT

A reliable operation and reducing the power consumption of the feed pumps of the ORC systems are highly important as the feed pump is one of the main components affecting the ORC power plant operating pressures, controllability, and the cycle net power output. Especially in small-scale and high -temperature ORC systems, the design of an efficient feed pump can be challenging because the required pressure increase over the pump is high and on the other hand, the working fluid flow rates are small. In this paper, the design and experimental investigation on the operation of a small-scale and high pressure ratio ORC feed pump are presented and analyzed. The investigated feed pump is of partial emission type and it is connected to a single shaft with a high-speed generator and a supersonic radial turbine. The design rotational speed of the turbogenerator is 31 000 rpm and the rated electric power output of the system is below 10 kW. The operation of the feed pump was investigated with different rotational speeds and under different flow rate conditions. In the experiments, the pump was capable to be operated at the target rotational speed range of 12 000 rpm to 31 000 rpm and the target pressure increase as well as the target working fluid flow rate were reached. This study presents the design method that was used for defining the partial emission pump geometry and analyses the operation of the pump under various operating conditions and rotational speeds. In addition, the methods for avoiding cavitation in this type of pumps are discussed. The results of the study shed light on the most important aspects in designing high pressure ratio – low flow rate feed pumps for ORC applications and discuss the specific operational characteristics of this type of pumps.

1 INTRODUCTION

Small-scale ORC systems have been intensively developed and investigated in the recent times for different applications. The efficient and reliable operation of feed pumps of small-scale ORC units is important for the operation of the whole power cycle. In this paper, a feed pump of a small-scale and high-temperature micro-ORC system is studied. The investigated high-speed ORC power plant has the main feed pump, turbine, and generator assembled on a single shaft. This solution allows to design ORC turbogenerators with a compact and hermetic structure. However, the combination of a low flow rate, high pressure increase, as well as low net positive suction head required makes a special pump design necessary with a requirement of high rotational speed for the studied application. As the main feed pump and the turbine are assembled on a single shaft the increase in shaft rotational speed directly affects the turbine operation, mass flow rate and pressure increase in the pump.

A displacement pump can be used but there are some down sides. One of them is oil lubrication which may be harmful for the process itself. A separate displacement pump may start to leak from the seals and the hermetic process may deteriorate.

One pump type that can be considered potential for low flow rate and high pressure increase applications is the partial emission (PE) pump, the PE pump mechanism is described in Section 2.2. Barske (1960) presented unconventional pump types including the PE pump. Mowrey (1988) discussed high head - low flow pump types, and one of those was a PE pump. In addition, a lightweight PE pump with generous clearances were needed to handle corrosive and contaminated rocket fuels. The partial emission construction can be used in compressor applications as well. Rodgers (1989) has presented

experiments with a single-stage, open face centrifugal partial emission compressor having a low non-dimensional specific speed of 0.15. In the experiments, a peak efficiency of 34% was gained.

In the later literature, Shao and Xhao (2019) made a numerical simulation for a PE pump based on the Reynolds-averaged Navier-Stokes equations combined with the RNG k-epsilon turbulence model. In their study, the calculated results were in accordance with the experimental data. Lee *et al.* (2016) used a numerical method for the optimum design process and made a CFD analysis to verify the theoretical performance of the PE pump.

In some earlier ORC processes built and tested at Lappeenranta University of Technology (LUT), a full emission type pump was used. This pump type has diffuser vanes in the rotor (so called rotating diffuser or covered wheel) and a vaneless stator. Later, due to the better cavitation characteristics and lower labyrinth seal leaks, PE type pumps have been used (van Buijtenen *et al.*, 2003). This pump type has diffusers on the stator named a so called partly blocked stator. The design and operating principles of a PE pump is presented in detail by Lobanoff and Ross (1992). Larjola *et al.* (1993) carried out experiments with a PE pump and formed analytical equations for the pump operation at the design operating condition. The investigated PE pump was designed by using the experimental results of Larjola *et al.* (1993) and the guidelines by Lobanoff and Ross (1992). In this paper, the design principles and the experimental results for the partial emission pump are presented and analyzed. The main equations and design principles are presented first. Then, the experimental data including different operating conditions are presented and analyzed. Finally, the conclusions and suggestions for the future work are presented.

2 DESIGN PROCESS

In the ORC process, the feed pump supplies the working fluid to the evaporator where the working fluid is heated and vaporized by the exhaust heat. This feed pump is a kinetic type PE pump. The pump design is made with the help of an inhouse code by Larjola *et al.* (1993) and Lobanoff and Ross (1992). The process diagram of the system is shown in Figure 1. The main feed pump receives fluid from the pre-feed pump. After the main feed pump the flow is divided into the bearing lubrication flow and into the flow going through the evaporator and turbine.

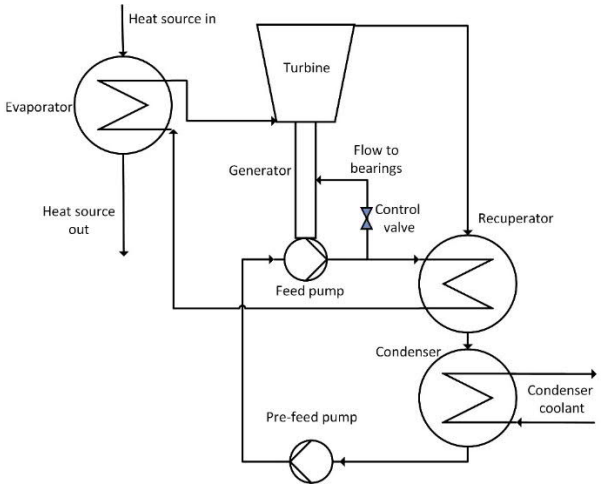

Figure 1: Process diagram of the Micro ORC

2.1 Process values

The pump design values are presented in Table 1. The working fluid is siloxane MDM and the fluid properties were calculated by using the commercial thermodynamic library Refprop. The more detailed description of the process layout and operating conditions are presented in Uusitalo *et al.* (2020).

Table 1: Pump design values

MDM fluid temp.	Pump inlet pressure	Pump mass flow/turbine mass flow	Pressure increase	Pump power	Design rotational speed *N*	Pressure increase in pre-feed pump
50 °C	0.23 bar.abs	0.37 kg/s/ 0.2 kg/s	10.3 bar	1.1 kW	31000 rpm	0.2 bar

2.2 Pump design

The net positive suction head available ($NPSH_A$) is important for reliable pump operation. $NPSH_A$ is given in equation (1). The lift loss, frictional loss and acceleration loss are ignored.

$$NPSH_A = \frac{p_{in}-p_v}{\rho g} + \frac{c_s^2}{2g} \quad (1)$$

where p_{in} is the absolute inlet pressure, p_v is the vapour pressure of the fluid, ρ is the fluid density, c_s is the velocity of the fluid in the inlet pipe, and g is the gravitational acceleration. Using the process design values, we get $NPSH_A$=2.7 m for the process.
Another important constant is the net positive suction head required, $NPSH_R$. In short, $NPSH_R$ implies to the suction pressure required by the pump for safe and reliable operation. $NPSH_R$ should be less than $NPSH_A$.

The properties of the kinetic pumps may be presented as a function of specific speed n_s and specific diameter d_s. These characteristic numbers describe the hydraulic features of a pump. The non-dimensional presentation forms are expressed in the following equations (Balje, 1981).

$$n_s = \frac{\omega\sqrt{q_v}}{\Delta h_s^{0.75}} = \frac{\omega\sqrt{q_v}}{\left(\Delta p/\rho\right)^{0.75}} = \frac{\omega\sqrt{q_v}}{(Hg)^{0.75}} \quad (2)$$

$$d_s = \frac{D\Delta h_s^{0.25}}{\sqrt{q_v}} = \frac{D\left(\Delta p/\rho\right)^{0.25}}{\sqrt{q_v}} = \frac{D\,(Hg)^{0.25}}{\sqrt{q_v}} \quad (3)$$

where D is the impeller diameter, q_v is the volumetric flow rate, ω is the angular velocity, Δp is the net pressure rise, Δh_s is the isentropic enthalpy rise, g is the gravitational acceleration, and H the is the head. Balje (1981) presents the $n_s d_s$ chart for various pump types. The $n_s d_s$ diagrams for PE pumps are also presented in (Balje, 1981). For PE pumps, the optimal choices are: n_s=0.05-0.3 and d_s=100-10. For typical centrifugal pumps, the optimal n_s value ranging from 0.2 to 2 is suggested (Balje, 1981). Figure 2 shows the principle and an example structure of a PE pump.

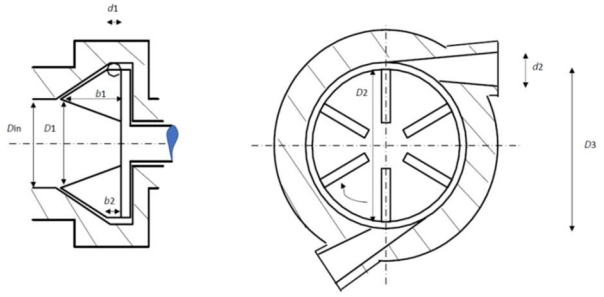

Figure 2: Low solidity, straight-vaned, radial "*Barske*" type partial emission pump

In the pump design for the LUT Micro ORC, two diffusers were chosen for the PE pump to compensate radial load for the hydrodynamic tilting pad bearings. The angle between the two diffusers is 150 °. The

value of the angle was selected due to possible flow vibration and minimizing radial load. In Table 2, the main design values of the PE pump of the Micro ORC setup are presented. The total mass flow through the pump is higher than the turbine mass flow because of the leaks through the labyrinth seals and the bearing lubrication flow. Figure 3 on the left presents the impeller of the pump.

Table 2: Design values of the PE pump

Pressure rise	**Head *H***	**Mass flow**	**n_s**	**d_s**	**η**	**P**	**Fluid density**	**Fluid vol. flow**
10.3 bar	134 m	0.37 kg/s	0.32	9.1	43 %	1.1 kW	780 kg/m^3	28.6 dm^3/min

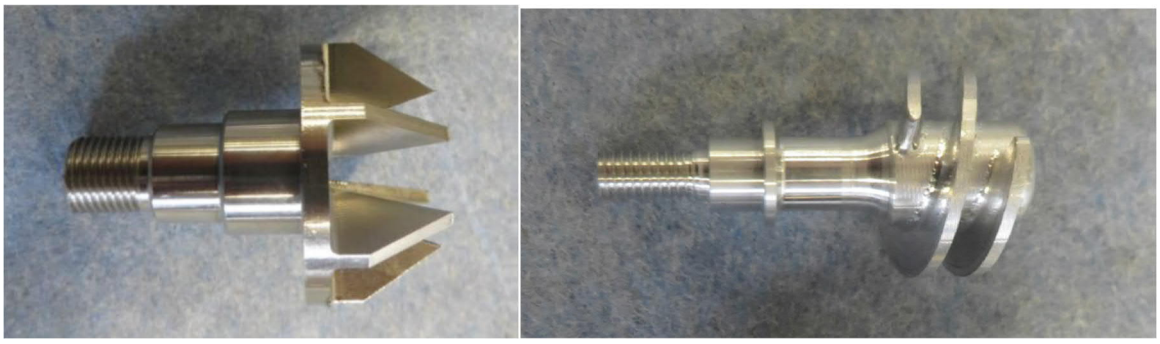

Figure 3: Impeller of the Micro ORC pump (left), (Uusitalo *et al.*, 2020), Inducer of the Micro ORC pump (right)

Lobanoff and Ross (1992) give an equation for the outer diameter D_2 and for the diffuser diameter d_1

$$D_2 = \frac{1300}{N}\sqrt{\frac{H}{\psi}} \quad (4)$$

$$d_1 = 0.268\sqrt{\frac{Q}{\varphi}}\left(\frac{\psi}{H}\right)^{0.25} \quad (5)$$

where ψ is the head coefficient (typically $\psi=Hg/U^2=0.74$, see Figure 4 right), and φ is the flow coefficient (typically $\varphi=U_{dif}/U=0.8$, see Figure 4 right) (Lobanoff and Ross, 1992). For calculation of the wheel outer diameter D_2 and the other main values, the experimentally derived equations were used (Larjola *et al.*, 1993). Pressure rise Δp can be calculated as (Larjola *et al.*, 1993)

$$\Delta p = \frac{1}{2}\rho(\omega_2 R_2)^2 + \frac{1}{2}\eta_d\rho(\omega_2 R_2)^2 \quad (6)$$

where ω_2 is the angular velocity of the fluid, and η_d is the recovery factor of the diffuser. The angular velocity of the fluid inside the pump ω_2 can be defined as

$$\omega_2 = k_1\omega. \quad (7)$$

Volumetric flow q_v can be solved as

$$q_v = k_2 n_{dif}\pi\left(\frac{d_1}{2}\right)^2\omega_2 R_2 \quad (8)$$

where n_{dif} is the number of the diffusers and d_1 is the diffuser diameter.
Coefficients k_1 and k_2 are defined as

$$k_1 = 1.055\left(1-\frac{1}{n_{bla}^{0.903}}\right)\left(1-\left(\frac{R_1}{R_2}\right)^{4.401}\right) \quad (9)$$

$$k_2 = 1.42\left(1-\frac{1}{n_{bla}^{0.49}}\right) \quad (10)$$

where n_{bla} is the number of the blades in the pump wheel. The solidity s is the ratio of the total blade length to the impeller circumference (Dahl, 1989)

$$s = \frac{Ln_{bla}}{\pi D_2} \tag{11}$$

where L is the impeller vane length, n_{bla} is the number of the impeller blades, and D_2 is the impeller outer diameter. Barske recommended from 2 to 6 blades of the wheel for adequate performance, but the later research suggests the number of blades greater than 20 having a significant positive effect on the performance (Dahl, 1989). Friction power P_f of the pump is (Larjola *et al.*, 1993)

$$P_f = \frac{1}{2}\rho\omega^3 R_3^4 (2k_3 R_3 + 2\pi b_2 k_4) \tag{12}$$

where R_3 is the stator radius and b_2 is the blade height of the wheel at the outer radius.
Coefficients k_3, k_4 and Reynolds number (Re) are defined as

$$k_3 = k_6 \frac{0.134}{\mathrm{Re}^{0.246}} \left(\frac{\bar{b}}{R_3}\right)^{0.0655} \tag{13}$$

$$k_4 = k_6 \frac{0.0105}{\mathrm{Re}^{0.193}} \tag{14}$$

$$\mathrm{Re} = \rho\omega_2 \frac{R_3^2}{\mu} \tag{15}$$

where $\bar{b}$ is the average blade height, k_6 is the roughness coefficient, and μ is the dynamic viscosity of the fluid. The efficiency of the pump can be calculated with equation

$$\eta = \frac{\Delta p q_v}{q_v \rho \omega R_2 \omega_2 R_2 + P_f} \tag{16}$$

An important dimensionless parameter in the pump design is known as suction specific speed S_s involving a parametric group nearly identical to the pump specific speed expression (Lobanoff and Ross, 1992).

$$s_s = \frac{\omega\sqrt{Q}}{(\mathrm{NPSH}_R)^{0.75}} \tag{17}$$

where Q is the volumetric flow and ω is the angular velocity. Typically, suction specific speed S_s for the PE pump is about 15 - 20 with input units [rad/s, m^3/s, m] (Lobanoff and Ross, 1992). High S_s values mean low $NPSH_R$, or good suction performance. Using S_s = 15, we can calculate $NPSH_R$ = 7.9 m for the PE pump.

Normally, this pump type has almost a constant head curve from zero flow to the design flow, see Figure 4 (Lobanoff and Ross, 1992). Increasing the flow from the design point, will significantly reduce the head. Decreasing the flow from the design point, the head vs. flow characteristic is prone to a “non-rising" curve toward the shutoff. This can weaken the stability at flow rates near the closing portion of the pump (Dahl, 1989). Table 3 presents the main dimensions of the investigated PE pump.

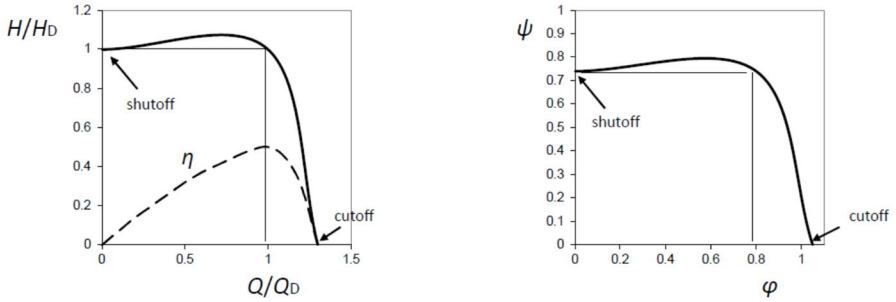

Figure 4: Performance trend of the PE pump (left), typical head coefficient (ψ) vs. flow coefficient (φ) for the PE pump (right)

Table 3: Main dimensions of the Micro ORC PE pump

Impeller outer diameter D_2	D_1/D_2 ratio	Number of blades in the wheel n_{bla}	Number of diffusers n_{dif}	Diffuser diameter d_1	Stator diameter D_3	Flow coeff. φ	Head coeff. ψ
33 mm	0.6	6	2	3 mm	36 mm	0.628	0.458

2.3 Inducer

In the earlier ORC projects at LUT, no inducer was used because cavitation was not expected, and $NPSH_A$ was in a safe level. With the pump design for MDM and with the cycle design parameters, cavitation is expected to be present. A more careful calculation revealed the necessity of using the inducer for this pump design. To reduce the required $NPSH_R$ an inducer was installed upstream of the pump impeller. The inducer boosts the inlet pressure of the pump and the risk of cavitation is thus reduced. The inducer was designed with the help of the work of Gülich (2014). Table 4 shows the main parameters for the inducer design, see Figure 3 right. According to the previous $NPSH_A$, pump impeller $NPSH_R$, and pre-feed pump head H_{pre}, the inducer should have head $H_{ind} = NPSH_R - NPSH_A - H_{pre} = 2.5$ m. The inducer design head, $H_{ind} = 3$ m was chosen for the pump design.

Table 4: Inducer details

Number of blades in inducer	Outer (tip) diameter	Inner (hub) diameter	Length	Number of turns
2	20 mm	10 mm	20 mm	2

2.4 Numerical simulation of the pump

The purpose of the numerical study presented in this section is to find out the possible risk of cavitation and to analyze flow fields in detail with CFD.

The pump operation at the design point was modelled with ANSYS CFX 2019 R3 using the mesh with 1.9 million elements, the SST k-omega turbulence model, inlet total pressure of 0.5 bar (abs.) and temperature of 60 °C, outlet static pressure of 10.8 bar (abs.), and rotational speed of 31 000 rpm. The material properties of MDM were read from a lookup table based on the NIST Refprop database. The pressure and velocity fields are presented in Figure 5. In the simulations, the mass flow rate close to the design value was gained. The results indicated low values of pressure near the shaft downstream from the inducer blades showing the flow region with the highest risk for cavitation. However, cavitation was not taken into account in the simulations as only the liquid phase was modelled. The results indicated also flow separation in the diffuser even though the computational domain outlet was located 35 mm downstream from the diffuser outlet.

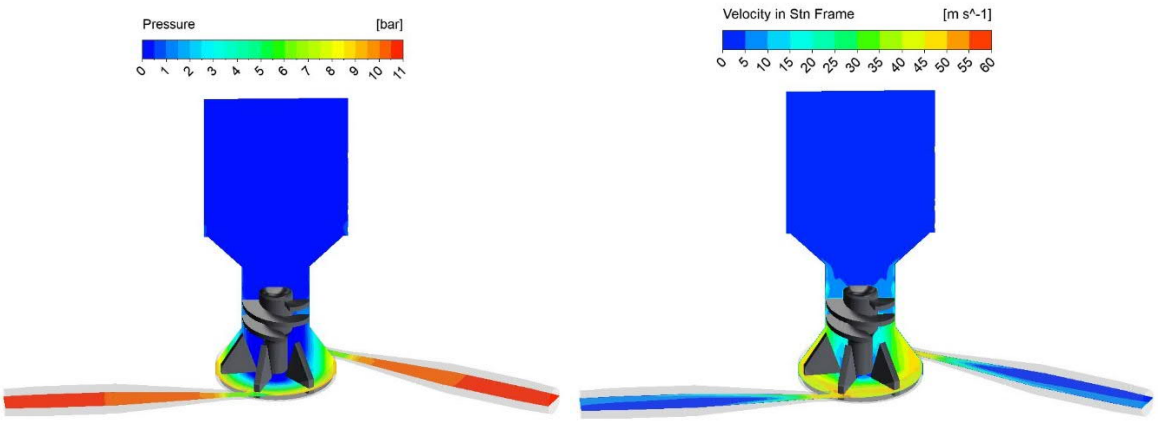

Figure 5: Calculated pressure distribution of the PE pump (left), velocity distribution of the PE pump (right)

3 TEST RESULTS

The pump has been tested under several operating conditions as a part of the full ORC test setup. The pump has been operated with different rotational speeds and with different flow rates through the pump. Experimental data of the pump outlet pressure vs. flow rate at different turbogenerator rotational speed ranges is shown in Figure 6 (left). The pressure before and after the pump were measured with commercial pressure transducers. The liquid flow rate at the pump inlet was measured by using a flow measuring flange having an orifice plate that was able to measure the flow rate through the pump from 0 kg/s up to 0.38 kg/s. At rotational speeds higher than 24 000 rpm the maximum value of the flange measurement was reached and thus, the data related to the highest rotational speeds is not included in the figure.
Figure 6 (right) shows the experimental data on rotational speed of the pump and pressure rise with the data categorized based on the turbogenerator speed ranging from 12 000 rpm to 31 000 rpm. The minimum allowable shaft speed (12 000 rpm) is due to the limitations in the liquid bearings at lower speeds.

In general, it has been observed that the investigated pump has been able to provide a sufficient pressure increase and flow rate with rotational speeds ranging from 12 000 rpm to 31 000 rpm. The higher is the TG rotational speed, the higher is the pressure increase and the working fluid flow rate through the pump. Conditions close to the pump design conditions including flow rate of 0.35 kg/s and pressure rise of 10 bar have been reached in the experiments. Most of the tested operating conditions have a lower pressure increase than the design value of 10 bar but a higher flow rate, as the turbine inlet pressure of 7-8 bar was targeted in most of the experimental runs. The variations in the pump outlet pressure and flow rate through the pump with respective rotational speeds were caused mainly by the different opening of the bearing flow control valve that divides the flow for the evaporator and for the turbogenerator bearings and affects the pump operating condition. In addition, the different process conditions and components, such as the evaporator heat rate, opening of the turbine valve and the turbine operating conditions were observed to have some impact on the pump operating point at different turbogenerator speeds. Cavitation was not observed.

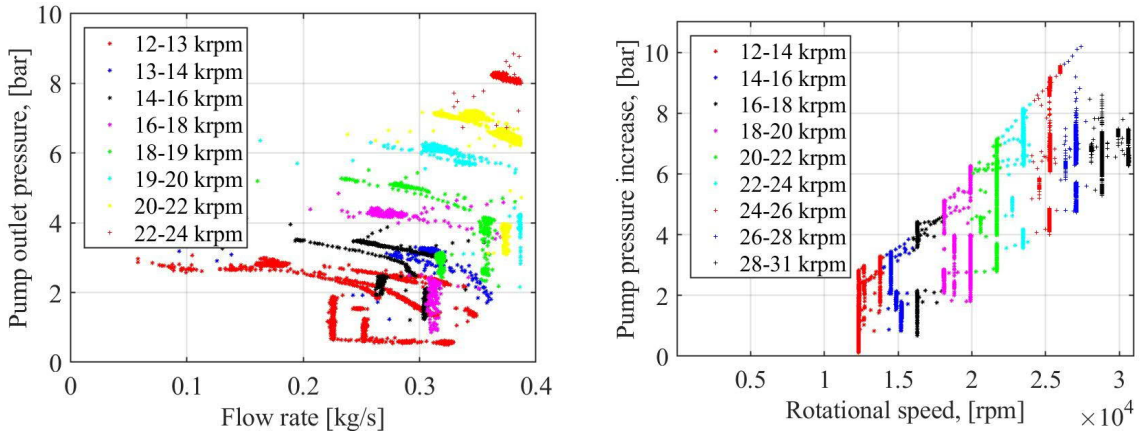

Figure 6: Pump outlet pressure vs. flow rate with different rotational speeds. The results are shown for turbogenerator rotational speed range of 12 000-24 000 rpm (left). Pump pressure increase as a function of turbogenerator rotational speed at rotational speed range of 12 000 rpm to 31 000 rpm (right)

4 CONCLUSIONS

In this paper, the design procedure of a partial emission pump operating as a feed pump of a small-scale and high pressure ratio ORC was presented. The methods for defining the pump geometry were presented and the methods for avoiding cavitation in this type of pumps were discussed. In addition, the CFD analysis for the pump design conditions and the experimental results on the pump operation were presented and analyzed. The investigated feed pump was connected to a single shaft with a high-speed generator and a supersonic radial turbine. The design rotational speed of the turbogenerator is 31 000 rpm and the rated electric power output from the system is below 10 kW.

In the experiments, the pump has been capable to be operated at the target rotational speed range of 12 000 rpm to 31 000 rpm and the target pressure increase as well as the target working fluid flow rate were reached. The results of the study shed light on the most important aspects in designing high pressure ratio – low flow rate feed pumps for ORC applications and discuss the specific operational characteristics of this type of pumps. In the future, more research on low flow rate - high pressure increase pumps, suitable for ORC systems is recommended to be carried out.

NOMENCLATURE

b_2	blade height, outer (m)
c_s	velocity in inlet pipe (m/s)
D	diameter (m)
d_1	diffuser diameter (m)
d_s	specific diameter (-)
H	head (m)
h_s	isentropic enthalpy (J/kg)
g	gravitational acceleration, 9.81 m/s^2
k	coefficient (-)
L	length of one impeller vane (m)
$NPSH_A$	Net Positive Suction Head Available (m)
$NPSH_R$	Net Positive Suction Head Required (m)
N	rotational speed (rpm)
n	number
n_{bla}	number of blades (-)
n_{dif}	number of diffusers (-)
n_s	specific speed (-)
p	pressure (Pa)
P	power (W)
P_f	friction power (W)
Q	volume flow (m^3/s)
q_m	mass flow (kg/s)
R_1	inner radius of the wheel (m)
R_2	outer radius of the wheel (m)
R_3	stator radius (m)
q_v	volume flow (m^3/s)
s	solidity (-)
S_s	suction specific speed (-)
U	speed (m/s)
v	velocity (m/s)

η	efficiency (-)
η_d	recovery factor (-)
ρ	density (kg/m^3)
μ	dynamic viscosity (Pa s)
ω	angular velocity (rad/s)
φ	flow coefficient (-)
ψ	head coefficient (-)

Subscript

2	outer
1	inner
abs	absolute
bla	blade
c	condenser
D	Design
dif	diffuser
g	gauge
in	inlet
ind	inducer
m	mass
pre	pre-feed pump
s	specific
v	volume; vapour
R	Required
A	Available

Abbreviations

MDM	octamethyltrisiloxane
ORC	Organic Rankine Cycle
PE	Partial Emission
TG	turbo generator

REFERENCES

Balje, O.E., 1981, *Turbomachines-A guide to Design, Selection, and Theory*, Son Wiley & Sons Inc. p. 513.

Barske, U.M., 1960, Development of some unconventional centrifugal pumps, *Proceedings of the Institution of Mechanical Engineers*, vol. 174, N:o 1, pp. 437-461.

van Buijtenen, J., Larjola, J., Turunen-Saaresti, T., Honkatukia, J., Esa, H., Backman, J., Reunanen, A. 2003, Design and validation of a new high expansion ratio radial turbine for ORC application, *5th European Conference on Turbomachinery*, Prague, March 2003.

Dahl, T., 1989, Centrifugal Pump Hydraulics for Low Specific Speed Applications, *Proceedings of the Sixth International Pump Symposium*, Texas A&M University, College Station, Texas, pp. 31-37.

Gülich, J.F., 2014, *Centrifugal pumps*, 3rd edition, Springer-Verlag Berlin Heidelberg 2014.

Jinwoo Lee, Yonghyun Kwon, Changhyeong Lee, Jungdong Choi, and Seokho Kim, 2016, Design of partial emission type liquid nitrogen pump, *Progress in Superconductivity and Cryogenics*, Vol.18, N:o 1, pp.64-68.

Larjola, J., Alamäki, J., Sallinen, P., Kytömäki, T., Esa, H., Seppänen, J., 1993, Suurnopeuspumput (in Finnish), Lappeenranta University of Technology, Department of Energy Technology, EN B-81, 50 p.

Lobanoff, V.S., Ross, R.R., 1992, *Centrifugal Pumps: Design and Application, 2nd edition*, Butterworth-Heinemann.

Mowrey, C.C., 1988, High Head – Low Flow Centrifugal Pumps, *Proceedings of the Fifth International Pump Symposium*, Texas A&M University, College Station, Texas, pp. 155-161.

Rodgers, C., 1989, Experiments with a Low Specific Speed Partial Emission Centrifugal Compressor, *ASME Gas Turbine and Aeroengine Congress and Exposition*, June 4-8, Toronto, Ontario, Canada.

Shao, X., Zhao, W., 2019, Performance study on a partial emission cryogenic circulation pump with high head and small flow in various conditions, *International journal of hydrogen energy*, 44, p. 27141-27150.

Uusitalo, A., Turunen-Saaresti, T., Honkatukia, J., Dhanasegaran, R., 2020, Experimental study of small scale and high expansion ratio ORC for recovering high temperature waste heat, *Energy, Vol. 208, 118321*.